npg

Activation of the transient receptor potential M2 channel and poly(ADP-ribose) polymerase is involved in oxidative stress-induced cardiomyocyte death

K-T Yang[1,5], W-L Chang[2,5], P-C Yang[3], C-L Chien[4], M-S Lai[4], M-J Su*,[2] and M-L Wu*,[1]

[1] Institute of Physiology, College of Medicine, National Taiwan University, Taipei, Taiwan
[2] Institute of Pharmacology, College of Medicine, National Taiwan University, Taipei, Taiwan
[3] Department of Internal Medicine, National Taiwan University Hospital, National Taiwan University, Taipei, Taiwan
[4] Institute of Anatomy and Cell Biology, College of Medicine, National Taiwan University, Taipei, Taiwan
[5] These authors equally contributed equally to this work
* Corresponding authors: M-L Wu, Institute of Physiology, College of Medicine, National Taiwan University, No. 1, Sec. 1, Jen-Ai Road, Taipei, Taiwan. Tel: + 886 2 23123456x8242; Fax: + 886 2 23224330; E-mail: mlw@ha.mc.ntu.edu.tw or M-J Su, Institute of Pharmacology, College of Medicine, National Taiwan University, No. 1, Sec. 1, Jen-Ai Road, Taipei, Taiwan. Tel: + 886 2 23123456x8317; Fax: + 886 2 23971403; E-mail: mjsu@ha.mc.ntu.edu.tw

Abstract

Overproduction of reactive oxygen species is one of the major causes of cell death in ischemic–reperfusion (I/R) injury. In I/R animal models, electron microscopy (EM) has shown mixed apoptotic and necrotic characteristics in the same cardiomyocyte. The present study shows that H_2O_2 activates both apoptotic and necrotic machineries in the same myocyte and that the ultrastructure seen using EM is very similar to that in I/R animal studies. The apoptotic component is caused by the activation of clotrimazole-sensitive, NAD^+/ADP ribose/poly(ADP-ribose) polymerase (PARP)-dependent transient receptor potential M2 (TRPM2) channels, which induces mitochondrial $[Na^+]_m$ (and $[Ca^{2+}]_m$) overload, resulting in mitochondrial membrane disruption, cytochrome c release, and caspase 3-dependent chromatin condensation/fragmentation. The necrotic component is caspase 3-independent and is caused by PARP-induced $[ATP]_i$/NAD^+ depletion, resulting in membrane permeabilization. Inhibition of either TRPM2 or PARP activity only partially inhibits cell death, while inhibition of both completely prevents the ultrastructural changes and myocyte death.
Cell Death and Differentiation (2006) **13,** 1815–1826.
doi:10.1038/sj.cdd.4401813; published online 18 November 2005

Keywords: mitochondrial Na^+ overload; TRPM2; PARP; apoptosis; necrosis

Abbreviations: TRPM2 channel, transient receptor potential M2 channel; ROS, reactive oxygen species; EM, electron

microscopy; I/R injury, ischemic–reperfusion injury; $[Na^+]_m$, mitochondrial Na^+ levels; $[Ca^{2+}]_m$, mitochondrial Ca^{2+} levels; CsA, cyclosporin A; PTP, permeability transition pore; cytC, cytochrome c; PARP, poly(ADP-ribose) polymerase; ADPR, ADP ribose; PAR, poly(ADP ribose); PARG, poly(ADP-ribose) glycohydrolase; NA, nicotinamide; 3-AB, 3-aminobenzamide; DPQ, 3,4-dihydro-5-[4-(1-piperidinyl)butoxy]-1(2H)-isoquinolinone; TUNEL, TdT-mediated dUTP-X nick end labeling; PI, propidium iodide; EthD-1, ethidium homodimer

Introduction

Overproduction of reactive oxygen species (ROS) is suggested to be responsible for myocyte death in ischemic–reperfusion (I/R) animal models and in patients with I/R injury.[1,2] Different types of myocyte death during I/R injury have been demonstrated, including apoptosis[2–4] and necrosis.[5,6]

The hallmarks of apoptosis are usually an intact membrane, chromatin condensation, and nuclear fragmentation.[7] The key events in the mitochondrial-dependent apoptotic pathway are the opening of the cyclosporin A (CsA)-sensitive permeability transition pore (PTP), resulting in the release of cytochrome c (cytC) and other apoptogenic proteins, and in caspase 3-dependent nuclear condensation/fragmentation.[4,8–10] ROS-induced mitochondrial Ca^{2+} ($[Ca^{2+}]_m$) overload is one of the major causes of PTP opening and cytC release, resulting in myocyte apoptosis.[4,11]

In contrast, necrosis is commonly characterized by an increase in plasma membrane permeability, release of intracellular proteins, and an absence of nuclear morphological changes.[7,12] One major hypothesis for I/R-induced necrotic cell death is that ROS-induced DNA damage results in excessive activation of the nuclear repair enzymes, the poly(ADP-ribose) polymerases (PARPs). The activated enzymes accelerate NAD^+ cleavage into poly(ADP ribose) (PAR), and the regeneration of NAD^+ consumes ATP; so the pools of both NAD^+ and ATP are depleted, leading to necrosis by energy depletion.[13] The use of PARP-1 null mice ($PARP^{-/-}$) or PARP inhibitors significantly reduces the I/R-induced infarct and peri-infarct (necrosis) area by ~20–25%.[13–15]

Electron microscopy (EM) shows that I/R-induced cell death does not result in a classic apoptotic or necrotic morphology, but in the appearance of both sets of characteristics in a single myocyte.[16–18] The ultrastructure changes include EM-TdT-mediated dUTP-X nick end labeling (TUNEL)-positive nuclear fragmentation, plasma membrane permeabilization, and mitochondrial hernia with loss of cristae. This untypical mode of cell death is not restricted to cardiac cells, as it is also seen by EM in the rat brain cortex after cerebral artery occlusion.[19] However, the molecular

mechanism involved in this untypical cell death remains unclear.

Mammalian homologs of the *Drosophila* TRP channel gene encode a family of at least 21 ion channel proteins. The TRP family mainly consists of Ca^{2+} channels and can be divided into three subfamilies: classic (TRPC) channels, vanilloid receptor-like (TRPV) channels, and melastatin-like (TRPM) channels.[20,21] Transient receptor potential M2 channel (TRPM2) (previously LTRPC2 or TRPC7) is a Na^+- and Ca^{2+}-permeable nonselective cation channel and can be activated by exposing TRPM2-expressing cell lines to H_2O_2.[22–24] ADP ribose (ADPR) is suggested as a downstream messenger for TRPM2 opening, since one domain of TRPM2, which is homologous to NUDT9 ADR hydrolase, binds ADPR.[25] However, it has also been suggested that NAD^+ directly gates the channel,[22,26] since ^{32}P-labeled β-NAD^+ binds strongly to the C-terminus of TRPM2.[22]

Here, we show that oxidative stress (20–100 μM H_2O_2) also induces both modes of cell death in a singe cultured rat cardiomyocyte and that the ultrastructure changes are similar to those seen in I/R animal models. The H_2O_2-induced apoptotic changes involve TRPM2 opening, which results in mitochondrial $[Na^+]_m$ (and $[Ca^{2+}]_m$) overload, followed by mitochondrial membrane disruption, cytC release, and caspase 3-dependent nuclear condensation/fragmentation, while the necrotic changes are caspase 3-independent, but PARP-dependent. Interestingly, inhibition of both TRPM2 and PARP activities totally abolishes H_2O_2-induced myocyte death.

Results

In the Supplementary Information, we show that functional TRPM2 channels are present in primary ventricular myocytes (Supplementary Figures S1 and S2). Since the electrophysiological properties of the H_2O_2-induced currents (Supplementary Figure S3) were very similar to those of the TRPM2 channel, the H_2O_2-induced $[Na^+]_i/[Ca^{2+}]_i$ overload (Supplementary Figure S3Ae–g) could result from TRPM2 opening. If this were the case, the endogenous levels of NAD^+ and/or ADPR should be raised by exposure to H_2O_2. We tested this hypothesis in Figure 1.

H_2O_2 increases intracellular levels of NAD^+ and ADPR

The fluorescence of reduced pyridine nucleotides (NADH and NADPH) accounts for most of the cellular autofluorescence seen on excitation at 340 nm, as oxidized pyridine nucleotides (NAD^+ and $NADP^+$) are nonfluorescent.[27] The basal level of NAD(P)H was normalized as $F/F_0 = 1$ ($F_0 =$ basal fluorescence; Figure 1Ad). When cells were exposed to 100 μM H_2O_2, the NAD(P)H levels started to decrease (i.e. NAD^+ levels increased) at 1.9 ± 0.2 min, and maximum NAD^+ levels were seen at 7.3 ± 0.8 min (Figures 1Ad and D). When H_2O_2 was continuously present for 60 min, there was no recovery of NAD(P)H (Figure 1Cb), indicating that NAD^+ is probably depleted at this time-point, since $[ATP]_i$ was depleted by exposure to 100 μM H_2O_2 for 60 min (see below). When rotenone was added in the continued presence of H_2O_2, NAD(P)H levels reversed rapidly (Figure 1Ac, d and D), as rotenone inhibits complex I in the respiratory chain, causing maximal accumulation of NAD(P)H.[27] Addition of rotenone alone had little effect (Figure 1D). The $OH^\bullet$ inhibitors, phenanthroline (Figure 1B and D) and DMTU (10 mM, not shown), completely inhibited the oxidation of NAD(P)H caused by H_2O_2, indicating that $OH^\bullet$ induced an increase in NAD^+ levels (Figure 6).

Application of a PARP inhibitor, 3-aminobenzamide (3-AB), for $\sim$40 min (Figure 1C) resulted in a small, but nonsignificant ($P > 0.05$; Figure 1C), reduction in basal levels of NAD(P)H, indicating that little PARP was activated under basal conditions. However, in the presence of H_2O_2, 3-AB induced partial recovery of NAD(P)H (Figure 1Cc), probably as a result of NAD^+ accumulation due to PARP inhibition, thus shifting the $NAD^+ \leftrightarrow NADH$ equilibrium to the right (Figure 6). Prevention of H_2O_2-induced NAD^+ depletion by PARP inhibitors has also been demonstrated in other studies.[28,29]

After treatment with DNA-damaging reagents (e.g. H_2O_2), the enzyme poly(ADP-ribose) glycohydrolase (PARG) converts PAR (half-life of less than 1 min) into mono(-ADPR).[13,30,31] Since anti-PAR antibody only recognizes the polymer,[32] to prevent PAR degradation into ADPR, the cells were fixed with trichloroacetic acid (see Supplementary Methods). Compared to the untreated control (Figure 1Ea), a marked increase in nuclear PAR immunoreactivity was seen in myocytes exposed for 5–20 min to 20 or 100 μM H_2O_2 (Figure 1Eb–d), the immunoreactivity decreasing after 30 min exposure (Figure 1Ed). Moreover, phenanthroline, rotenone, 3,4-dihydro-5-[4-(1-piperidinyl)butoxy]-1(2H)-isoquinolinone (DPQ), or 3-AB largely inhibited the PAR formation seen after 20 min exposure to 100 μM H_2O_2 (Figure 1Ed), indicating that these chemicals effectively prevented PARP-activated PAR formation. The above results (Supplementary Figures S1–S3 and Figure 1) therefore indicate that the TRPM2 may be activated by H_2O_2-induced NAD^+/ADPR formation (see Discussion), resulting in the $[Na^+]_i$ and $[Ca^{2+}]_i$ overloads.

ROS-induced mitochondrial Ca^{2+} ($[Ca^{2+}]_m$) overload is one of the major causes of myocyte apoptosis.[4,11,33] Since we found that 50% of the $[Ca^{2+}]_i$ overload originated from the

Figure 1 H_2O_2 increases intracellular levels of NAD^+ and PAR, and 3-AB (a PARP inhibitor) partially recovers NADH levels. (**A**) (**a–d**) After addition of 100 μM H_2O_2 to the bath solution, NAD^+ levels increase (i.e. NADH levels decrease) rapidly and the response is reversed by addition of 10 μM rotenone ($n = 5$). The basal level of NAD(P)H is normalized as $F/F_0 = 1$ (**d**). (**B**) Phenanthroline (1 mM, 30 min pretreatment) completely inhibits the increase in NAD^+ levels during exposure to H_2O_2 ($n = 4$). (**C**) (**a**) 3-AB (1 mM) alone has a small, but nonsignificant, effect ($P > 0.05$, 1**d**) on basal NADH levels. (**b, c**) In the continuous presence of H_2O_2 for 60 min, there is no NADH recovery ($n = 4$), while early addition of 3-AB partially recovers the level of NADH (see text). (**D**) Statistical analysis of the data from (**A**)–(**C**). (**E**) (**a**) Control, (**b–c**) PAR immunoreactivity (see Supplementary Methods) in the nucleus ('Nu') after 20 min exposure to 20 μM or 100 μM H_2O_2. (**d**) Time-course of changes in PAR after exposure to 100 μM H_2O_2. Note that a very low concentration of H_2O_2 (20 μM) causes an increase in PAR, while phenanthroline (1 mM), 3-AB (1 mM), DPQ (30 μM), or rotenone (10 μM) markedly inhibits PAR formation at 20 min exposure. After exposure to H_2O_2 for 60 min, cells were washed ('wash' in **Ed**) and returned to normal medium. At least four animal preparations were used ($n = 4$), each tested in duplicate (**D** and **Ed**)
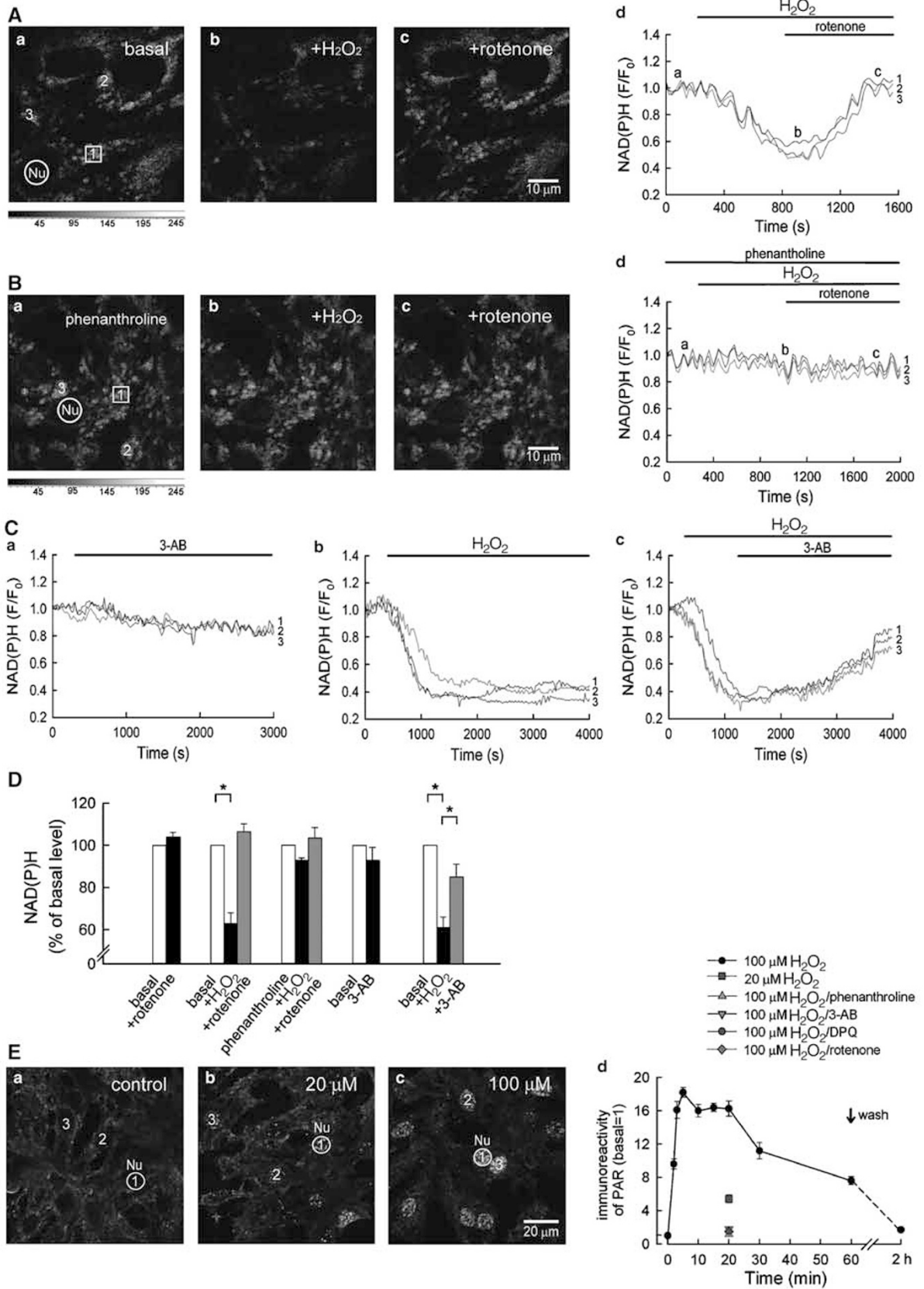
H_2O_2-induced $[Na^+]_i$ overload (Supplementary Figure S3Ae–g), a possible role of $[Na^+]_{cyt}/[Na^+]_m$ overload in myocyte death was investigated in detail.

Mitochondrial Na^+ ($[Na^+]_m$), but not cytosolic Na^+ ($[Na^+]_{cyt}$), overload is involved in the H_2O_2-induced caspase 3-dependent apoptotic pathway

CoroNa Red has been used to measure changes in cytosolic Na^+ ($[Na^+]_{cyt}$).[34] Using confocal microscopy with a thin optical section (0.04 µm), it can be used to simultaneously report changes in the $[Na^+]_{cyt}$ and $[Na^+]_m$, since only a small proportion of the probe is found in the cytosolic compartment,[34] the majority being trapped by the negative mitochondrial potential because of the positive charge of the probe. Since the nuclear membrane is no barrier to cytosolic ion movement,[35,36] averaging the signal over a small nuclear optical section (ER-free and mitochondria-free) or the mitochondria (identified by a mitochondrial marker, MTG, last frame in Figures 2a and c), respectively, allows dynamic changes in the $[Na^+]_{cyt}$ or $[Na^+]_m$ to be recorded.

After exposure to 100 µM H_2O_2 for 680 s in normal medium (Figures 2a and e, Video Supplementary Figure S1) or after clamping the $[Na^+]_i$ at 60 mM using Na-ionophore cocktail (5 µM gramicidin D, 40 µM monensin, and 100 µM strophanthidine) in Ca-free medium,[33] the peak levels of $[Na^+]_{cyt}$ and $[Na^+]_m$ were ~60 mM (Figure 2e). Photobleaching of CoroNa Red did not occur, since there was little change in the absence of H_2O_2 treatment ('-H_2O_2' in Figure 2b). Moreover, little H_2O_2-induced $[Na^+]_{cyt}/[Na^+]_m$ increase was seen in Na-free medium, while Ca-free medium did not have any inhibitory effect (Figure 2e), indicating that the probe is Na-sensitive and Na-selective. Pretreatment with 10 µM RU360, a potent inhibitor of the mitochondrial Ca^{2+} import pathway,[37,38] markedly inhibited the H_2O_2-/Na-ionoph-induced $[Na^+]_m$ overload, but not the $[Na^+]_{cyt}$ overload (i *versus* ii in Figures 2c and e), showing that RU360 effectively prevents $[Na^+]_m$ overload.

Significant chromatin condensation (arrows in Figure 2fi) and DNA fragmentation (Figure 2fii, green for TUNEL (+) staining) were seen after 4.5 h wash-out of H_2O_2 or of Na-ionophore cocktail/Ca-free medium (Figure 2g). Approximately 18% inhibition of condensation was seen in Ca-free medium (Figure 2g), in which the $[Ca^{2+}]_m$ overload should be totally abolished. Moreover, treatment with RU360, Na-free medium, Z-DEVD.fmk (a specific caspase 3 inhibitor), or phenanthroline (an iron chelator that prevents $OH^•$ production; Figure 6) markedly inhibited not only H_2O_2-induced, but

also Na-ionophore-induced, chromatin condensation (Figure 2g), indicating that $[Na^+]_m$ overload *per se* plays an important role in caspase 3-dependent apoptosis.

Since ROS-induced $[Ca^{2+}]_i$ overload[39] and PARP activation[13] have been suggested to also induce necrosis, we tested whether $[Ca^{2+}]_i/[Na^+]_i$ overload and PARP activation were involved in the necrotic machinery.

PARP activation, but not $[Na^+]_i/[Ca^{2+}]_i$ overload per se, is involved in the H_2O_2-induced necrotic pathway

Two common indicators used to demonstrate necrosis are membrane permeabilization and release of cytosolic protein (e.g. calcein-AM).[12,40] After 60 min treatment with 100 µM H_2O_2, the cells were immediately incubated with a mixture of CAM (green) and ethidium homodimer (EthD-1) (red), then washed, fixed, and stained with a muscle marker, antibody A12 (blue). In the untreated cells, the live myocytes (blue) stained green for calcein (arrows in Figure 3a) and contained no red nuclei, while $78 \pm 5\%$ ($n = 6$) of the H_2O_2-treated cells showed red nuclear labeling (EthD-1, arrows in Figure 3b) and no calcein staining, confirming that H_2O_2 also induces necrosis. This raises the question whether the permeabilization of the plasma membrane is due to $[Ca^{2+}]_i$ and/or $[Na^+]_i$ overload. To our knowledge, this possibility has not been properly tested previously. Using time-lapse confocal microscopy of live myocytes, the temporal profiles of changes in the $[Ca^{2+}]_i$ (fluo 3-loaded cells) and membrane permeabilization (propidium iodide (PI) added to the external medium) were measured simultaneously.

When myocytes were treated with H_2O_2, a slow increase in the $[Ca^{2+}]_i$ was seen (green, Figure 3c). Extracellular PI did not enter the cell and stain the nuclei (red) until the fluo 3 had started to leak out slowly (Figure 3c, see video Supplementary Figure S2), indicating that the early Ca^{2+} influx (and Na^+ influx, not shown) was not due to membrane permeabilization. Moreover, the Ca^{2+} influx was completely inhibited by phenanthroline (an $OH^•$ inhibitor, Figures 3e and 6) but *partially* inhibited by DPQ (a PARP inhibitor) (Figure 3f). Importantly, the permeabilization was *independent* of $[Na^+]_i$ or $[Ca^{2+}]_i$ overload, since Ca-free (Figure 3g) or Na–Ca-free medium (Figure 3d) did not inhibit the PI influx.

The level of the $[ATP]_i$ has been suggested to be the switch deciding between apoptosis and necrosis, since the formation of the apoptosome in the caspase 3-mediated apoptotic pathway is dATP/ATP-dependent (Figure 6).[12] Since H_2O_2 induced both membrane permeabilization (Figure 3b and c)

Figure 2 $[Na^+]_m$ overload *per se* initiates caspase 3-dependent apoptosis. (**a, b**) H_2O_2 induces both $[Na^+]_{cyt}$ ('Nu', nucleus) and mitochondrial (Mt) Na^+ ($[Na^+]_m$) overload. See Supplementary Methods for measurement and transformation into $[Na^+]_{cyt}/[Na^+]_m$ (in mM). (**c–e**) Na-ionophore cocktail medium ('Na-ionoph') also induces $[Na^+]_{cyt}/[Na^+]_m$ overload (**e**) and RU360 selectively inhibits the H_2O_2-/Na^+ ionoph-induced $[Na^+]_m$ overload (i *versus* ii in **c**), but not the $[Na^+]_{cyt}$ overload (**d, e**). The Na^+ ionophore cocktail medium effectively clamps the $[Na^+]_i = [Na^+]_o$.[33] The Na-ionoph/Ca-free medium contained 5 µM gramicidin D, 40 µM monensin, and 100 µM strophanthidine in 60 mM NaCl-containing medium. Note that the Ca-free medium has little inhibitory effect on the H_2O_2-induced $Na^+_{cyt}/[Na^+]_m$ overload (**e**). (**f**) Cells were exposed to 100 µM H_2O_2 for 60 min, then returned to normal medium for 4.5 h; the nucleus shows chromatin condensation (arrows in **i**, Hoechst staining) and DNA fragmentation (**ii**) (green or blue for TUNEL or myocyte staining, respectively; see Supplementary Methods). (**g**) Prevention of $[Na^+]_m$ overload by RU360 inhibits the caspase 3-dependent apoptosis. In Ca-free medium, there is an ~18% inhibition of the nuclear condensation. The Na-ionoph/Ca-free medium was exposed for 30 min and wash-out for 4.5 h. H_2O_2 (100 µM), Z-DEVD.fmk (100 µM, 2 h pretreatment, a caspase 3 inhibitor), phenanthroline (1 mM, 30 min pretreatment), and RU360 (10 µM, 2 h pretreatment) were used. All results are expressed as the mean ± S.E.M. for at least four animal preparations ($n = 4$), each tested in duplicate. In all, 200 cells from 10 randomly selected fields were scored on each coverslip. *$P < 0.05$ compared, respectively, to the H_2O_2 group or Na-ionoph group as appropriate
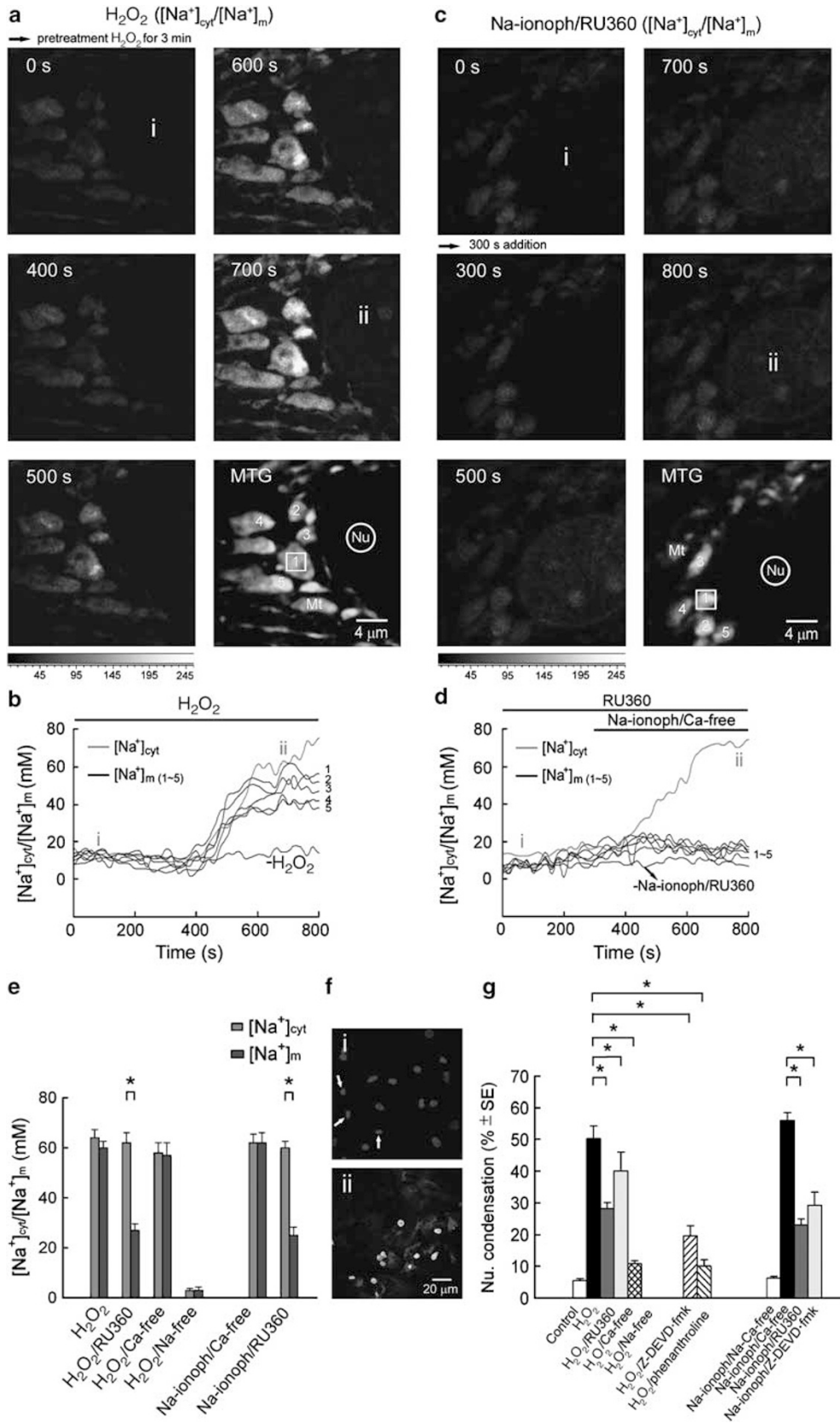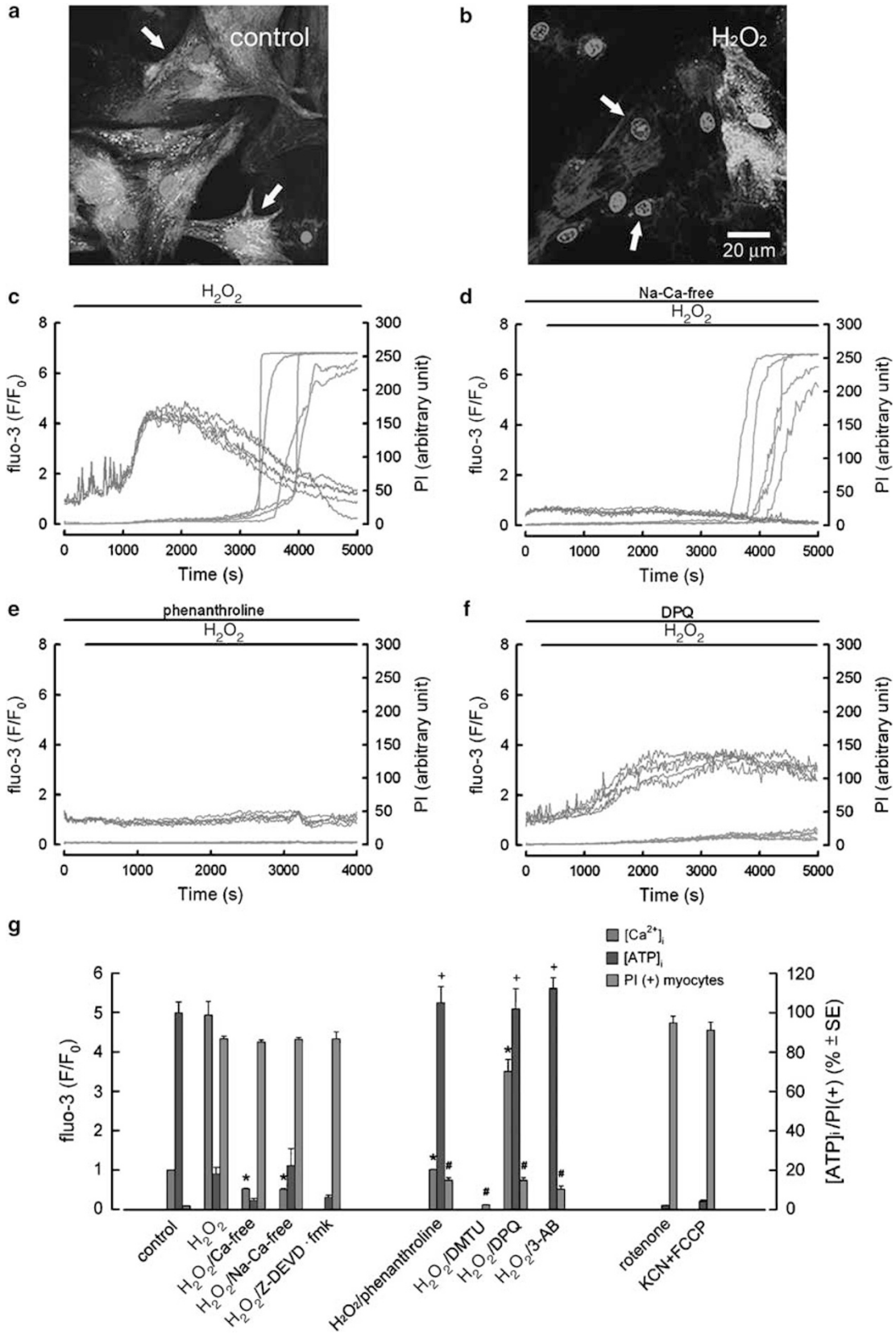
and caspase 3-dependent nuclear condensation (Figure 2g), the $[ATP]_i$ was measured. After 60 min treatment with 100 μM H_2O_2 in normal medium, Ca-free medium, or Na–Ca-free medium, or with chemical ischemia (rotenone or KCN/FCCP), the $[ATP]_i$ markedly decreased and PI staining increased (Figure 3g). Inhibition of OH$^\bullet$ production (phenanthroline or DMTU) or of PARP activation (DPQ or 3-AB) prevented the H_2O_2-induced $[ATP]_i$ depletion and increase in PI staining (i.e. membrane permeabilization; Figure 3g). Importantly, the membrane permeabilization and $[ATP]_i$ depletion were not inhibited by a specific caspase 3 inhibitor, Z-DEVD.fmk (Figure 3g), suggesting that OH$^\bullet$ induced PARP activation (Figure 6), via a *caspase 3-independent* necrotic pathway.

We next investigated the molecular mechanisms for the caspase 3-dependent and caspase 3-independent cell death.

Mechanisms for activation of both apoptotic and necrotic machineries in a single myocyte

H_2O_2-induced Na$^+$ or Ca^{2+} influx was monitored by recording changes in the $[Na^+]_i$ (using SBFI-AM) or $[Ca^{2+}]_i$ (using fura 2-AM) (Supplementary Methods). When cells were exposed to 20–500 μM H_2O_2 for 20–25 min, there was a parallel increase in the $[Na^+]_i$ and $[Ca^{2+}]_i$ (Figure 4a). Since a smaller inhibitory effect on nuclear condensation was seen under Ca-free conditions than under Na-free conditions (Figure 2g), Na-free medium was used when different concentrations of H_2O_2 (20–500 μM) were applied (brown line in Figure 4b). We found that, even at a *low H_2O_2 concentration* (20 μM), inhibition of $[Na^+]_i/[Na^+]_m$ overload largely inhibited condensation (measured at 4.5 h wash-out, brown *versus* black in Figure 4b). Moreover, an increase in the H_2O_2 concentration (20–500 μM H_2O_2 exposure for 60 min) resulted in a decrease in the $[ATP]_i$ and an increase in membrane permeability PI (+) staining (Figure 4b).

A constant concentration of 100 μM H_2O_2 was then used to explore the temporal relationship between $[ATP]_i$ depletion, membrane permeabilization, caspase 3 activation, and nuclear condensation. After 40 min of H_2O_2 exposure, the $[ATP]_i$ was reduced to ~20% of control levels (blue, Figure 4c) and this was *followed* by a rapid increase in PI staining (red) at 60 min (Figures 3c and 4c; see video Supplementary Figure S2), indicating that depletion of $[ATP]_i$ may increase the membrane permeability, as suggested by other studies.[12,13] However, marked caspase 3 activation (green) was already seen at 20 min (Figure 4c), that is, earlier than $[ATP]_i$ depletion and PI influx. Chromatin condensation was not seen until after 2 h of wash-out of H_2O_2 (arrows, Figure 4ci), then increased with time. Furthermore, all
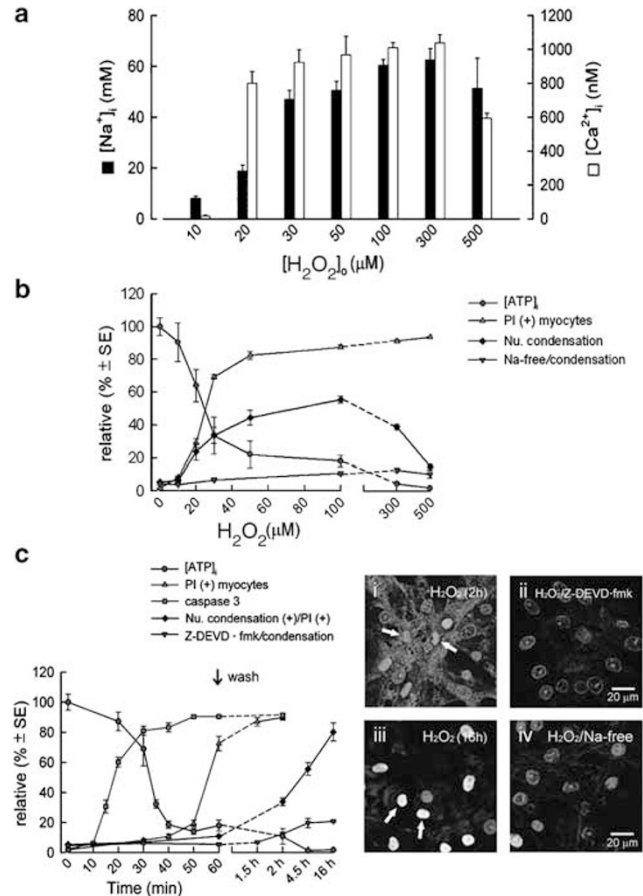

Figure 4 H_2O_2 evokes two modes of cell death in the same myocyte via caspase 3-independent membrane permeabilization and Na-sensitive, caspase 3-dependent nuclear changes. (**a**) Dose–response for the peak level of the H_2O_2-induced $[Na^+]_i$/$[Ca^{2+}]_i$ overload after exposure to 10–500 μM H_2O_2 ($n = 6$ for each group). The $[Na^+]_i$ or $[Ca^{2+}]_i$ were measured by SBFI-AM or fura 2-AM, respectively (see Supplementary Methods). (**b**) Changes in $[ATP]_i$ (see Supplementary Methods), membrane permeability (PI staining), nuclear condensation after 60 min exposure to 10–500 μM H_2O_2 ($n = 5$). $[ATP]_i$ and PI staining were immediately measured after H_2O_2 treatment. Na-sensitive nuclear condensation (black *versus* brown, Hoechst staining) was measured after 4.5 h wash-out of 10–500 μM H_2O_2 (exposure for 60 min). (**c**) Time-course of changes in $[ATP]_i$ (blue), PI staining (red), caspase 3 activation (green), and Z-DEVD.fmk (brown)-sensitive chromatin condensation after exposure to 100 μM H_2O_2. Cells were exposed to 100 μM H_2O_2 for 60 min, followed by wash-out (red arrow) for 1.5–16 h. The black line in (**c**) is the myocyte, which is stained positively for both nuclear condensation and PI within one cell. (**c**) (**i**) Caspase 3 activation (green), nuclear condensation (arrows), and membrane permeabilization (red) are seen in the same myocyte after 2 h wash-out of H_2O_2. (**ii**) Caspase 3 activation and nuclear condensation, but not membrane permeabilization, are markedly inhibited by 100 μM Z-DEVD.fmk. (**iii**) After 60 min treatment with H_2O_2, followed by 16 h wash-out, myocytes show double labeling (yellow) for TUNEL (green, DNA fragmentation) and PI (red). (**iv**) Na-free medium markedly inhibits H_2O_2-induced DNA fragmentation, but not membrane permeabilization, indicating an antiapoptotic effect at least for 16 h using Na-free medium (see Supplementary Methods for staining)

Figure 3 PARP activation is involved in the H_2O_2-induced $[ATP]_i$ depletion and membrane permeabilization, which are both caspase 3-independent. (**a**) Controls (arrows). (**b**) The membrane permeability increases after 60 min exposure to 100 μM H_2O_2. Membrane permeabilization (EthD-1 (+) staining) is shown by the arrows, stained with calcein (green), EthD-1 (red), and antibody A12 (blue). (**c–f**) Time-lapse recordings of H_2O_2-induced Ca^{2+} influx (measured by fluo 3 AM, see Supplementary Methods), followed by PI influx (membrane permeabilization) in live myocytes ($n = 4$, see also video Supplementary Figure S2). Phenanthroline (1 mM) completely, and DPQ (30 μM) partially, inhibits the Ca^{2+} influx (both $n = 4$). (**g**) Summary histograms for the peak $[Ca^{2+}]_i$ response (green, data from **c–f**) and $[ATP]_i$ (blue) and PI staining (red) after various treatments. Ca-, Na–Ca-free, or Z-DEVD.fmk (100 μM, a caspase 3 inhibitor) has little inhibitory effect on $[ATP]_i$ depletion and membrane permeabilization, while PARP inhibitors (1 mM 3-AB and 30 μM DPQ) or OH$^\bullet$ scavengers (1 mM phenanthroline and 20 mM DMTU) abolish both effects. The concentrations of rotenone, KCN, or FCCP were 10 μM, 5 mM, or 1 μM, respectively. $[ATP]_i$ and PI staining were measured immediately after 60 min treatment. All results are expressed as the mean ± S.E.M. for at least five animal preparations ($n = 5$), each tested in duplicate. $^{*+\#}P < 0.05$, compared to the H_2O_2-induced $[Ca^{2+}]_i$ increase (*), $[ATP]_i$ depletion ($+$), and membrane permeabilization (PI(+), $\#$) as appropriate

condensed nucleus (Hoechst staining) was also stained by PI (black, Figure 4c). After 16 h of wash-out, for example, the same nucleus in 80% of myocytes was stained with both TUNEL (DNA fragmentation) and PI (yellow, Figure 4ciii). Again, Na-free medium largely prevented TUNEL staining (yellow; Figure 4civ), but not PI staining (red), confirming that the membrane permeabilization seen in Figure 3g was $[Na^+]_i$-independent. Importantly, caspase 3 activation (green), chromatin condensation (arrows), and PI staining (red) were all seen within the same myocyte (Figure 4ci), indicating that both modes of cell death were induced by H_2O_2 in the same cell. Z-DEVD.fmk did not inhibit PI staining (Figure 4cii), but abolished both caspase 3 activation (Figure 4ci *versus* cii) and chromatin condensation (brown line in Figure 4c), indicating that the nuclear condensation, but not the membrane permeabilization, was caspase 3-dependent.

These results show that both TRPM2-induced $[Na^+]_m$ (and $[Ca^{2+}]_m$) overload and PARP-dependent $[ATP]_i$ depletion are important in the induction of the untypical cell death (Figure 6). We next tested whether the simultaneous inactivation of both the TRPM2 and PARP conferred a better protective effect.

Inhibition of both TRPM2 opening and PARP activation prevents both modes of cell death

Since both NAD^+ and ADPR are suggested to be specific messengers for TRPM2 opening, we manipulated endogenous levels of NAD^+ and/or ADPR or directly inhibited the TRPM2, then examined (i) whether NAD^+ and/or ADPR were involved in the H_2O_2-/TRPM2-induced Na^+/Ca^{2+} influx, and (ii) whether simultaneous inhibition of both TRPM2 and PARP activity prevented both modes of cell death.

Phenanthroline or rotenone, which inhibited the increase in levels of *both* NAD^+ and PAR/ADPR (Figures 1B, E, and 6), or clotrimazole, a putative TRPM2 inhibitor (Supplementary Figure S2Ab), completely inhibited the H_2O_2-induced Na^+ influx (Figure 5A and C) and Ca^{2+} influx (not shown), resulting in rapid recovery from $[Na^+]_i$ overload in the absence of an Na–K ATPase inhibitor. However, 3-AB/DPQ, which completely inhibited the increase in PAR/ADPR levels (Figure 1Ed) while partially restoring $NADH/NAD^+$ levels (Figure 1Cc), had a small inhibitory effect on both the $[Ca^{2+}]_i$ overload (Figures 3f and 5B) and the $[Na^+]_i$ overload ($33 \pm 5\%$ for 3-AB, $n = 4$), indicating that both NAD^+ and ADPR are involved in the

TRPM2 opening. Thus, PARP activation contributes not only to membrane permeabilization but also to TRPM2 opening.

Direct inhibition of TRPM2 by clotrimazole did not inhibit the H_2O_2-induced membrane permeabilization (red bar in Figure 5Giii), but almost completely abolished cytC release (Figure 5D), caspase 3 activation (green fluorescence in Figure 5Ei; Figure 5Eii: red for myocyte marker), and nuclear condensation/fragmentation (Figure 5F and green bar in Figure 5Giii), indicating that TRPM2 activation is involved in the apoptotic process. Z-DEVD.fmk markedly abolished the nuclear condensation (Figure 2g) and TUNEL response (green bars in Figure 5Giii), but not the EthD-1 staining (red bar in Figure 5Giii), again suggesting that DNA fragmentation/condensation, but not membrane permeabilization, is caspase 3-dependent. In contrast, inhibition of PARP activity by 3-AB or DPQ completely abolished membrane permeabilization (red bars in Figure 5Giii), but only had a weak inhibitory effect on condensation/fragmentation (15–20%; Figure 5F and Giii). These results therefore suggest that both TRPM2 opening and PARP activation are involved in the cell death. Simultaneous inhibition of TRPM2 and PARP almost completely abolished both the apoptotic (TUNEL staining) and necrotic features (EthD-1 staining, blue for myocyte marker in Figure 5Gii and Giii).

When examined by EM, myocytes exposed to 100 μM H_2O_2 for 60 min (Figure 5Hb) showed disruption of membrane integrity (arrows) and mitochondrial hernia and loss of cristae (arrow heads). Little change in chromatin was seen after 60 min exposure to H_2O_2 (Figure 5Hb, see the red nucleus in Figure 3b), but chromatin fragmentation was more obvious after 4.5 h (inset, see TUNEL staining in Figure 2fii). These ultrastructure changes were very similar to those seen in the infarct/peri-infarct zone in I/R animal studies.[16–18]

It has been suggested that PTP opening induces water influx, resulting in disruption of the outer mitochondrial membrane (OMM, i.e. hernia), followed by cytC release.[4,10] The present study showed that the use of Na-free medium largely prevented H_2O_2-induced mitochondrial hernia formation and loss of cristae (arrow heads, Figure 5Hc), but did not protect the plasma membrane (arrows), suggesting that the H_2O_2-/TRPM2-induced $[Na^+]_m$ overload (Figures 2a, 5A and C) was important in OMM disruption and clotrimazole-sensitive cytC release (Figure 5D). Cotreatment with 3-AB (PARP inhibition) and clotrimazole (inhibition of both Na^+/Ca^{2+} influx) markedly prevented the mitochondrial swelling,

Figure 5 Inhibition of both TRPM2 opening and PARP activation prevents both apoptotic and necrotic features. (**A**, **C**). In the absence of an Na–K ATPase inhibitor, 1 mM phenanthroline (30 min pretreatment, $n = 4$), rotenone (10 μM, $n = 5$), or clotrimazole (50 μM, $n = 5$) completely abolishes H_2O_2 (100 μM)-induced Na^+ influx and accelerates recovery from $[Na^+]_i$ overload. (**B**) Pretreatment with PARP inhibitors, 3-AB (1 mM), or DPQ (30 μM), partially inhibits the $[Ca^{2+}]_i$ overload – 33 ± 5% for 3-AB, 27 ± 5% for DPQ, both $n = 5$. (**D**, **E**) The H_2O_2-induced cytC release (**D**) and caspase 3 activation (green fluorescence, **Ei**) are completely inhibited by 50 μM clotrimazole ($n = 5$), a putative TRPM2 inhibitor. CytC release and caspase 3 activation were measured immediately after 100 μM H_2O_2 exposure for 60 min. (**F**) Clotrimazole almost completely inhibits nuclear condensation ($n = 5$), while 3-AB or DPQ inhibits condensation by ~15–20% ($n = 4$). (**G**) (**i**, **ii**) Myocytes (blue) staining with both TUNEL (green, DNA fragmentation) and EthD-1 (red, membrane permeabilization) are shown with yellow nuclei and was abolished by cotreatment with clotrimazole and DPQ. (**iii**) After simultaneous inhibition of both TRPM2 and PARP activity by cotreatment with clotrimazole ($n = 5$) and DPQ ($n = 4$) or 3-AB ($n = 6$), H_2O_2-induced DNA fragmentation (TUNEL, green) and membrane permeabilization (EthD-1, red) are markedly inhibited. Note that Z-DEVD.fmk (100 μM) inhibits the TUNEL response, but not membrane permeabilization ($n = 5$). Nuclear condensation and fragmentation were measured after 4.5 h (**F**, **G**) wash-out of H_2O_2. (**H**) Electron micrographs. (**a**) control, (**b**) an increase in plasma membrane permeability (black arrows) and mitochondrial (Mt) hernia and loss of cristae (arrow heads) are seen after 60 min exposure to 100 μM H_2O_2. Inset: chromatin condensation/fragmentation is more obvious at 4.5 h. (**c**) Na-free medium prevents the hernia (i.e. breakdown of the OMM, arrow heads) without preventing the mitochondrial swelling or protecting the plasma membrane (arrows). (**d**) Cotreatment with 3-AB and clotrimazole markedly prevents membrane permeabilization (arrows), OMM rupture (arrow heads), and chromatin fragmentation (measured at 4.5 h after wash-out of H_2O_2)

OMM disruption (arrow heads), plasma membrane permeabilization (arrows in Figure 5Hb), and chromatin fragmentation normally seen after 4.5 h exposure to H_2O_2 (inset, Figures 2fii and 5Hb), again showing that activation of both TRPM2 and

PARP was involved in the generation of the mixed features of cell death (Figure 6). However, mitochondrial swelling was not abolished in H_2O_2/Na-free medium (Figure 5Hc), possibly because a $[Ca^{2+}]_i$ overload ($\sim$500 nM, $\sim$50% inhibition by
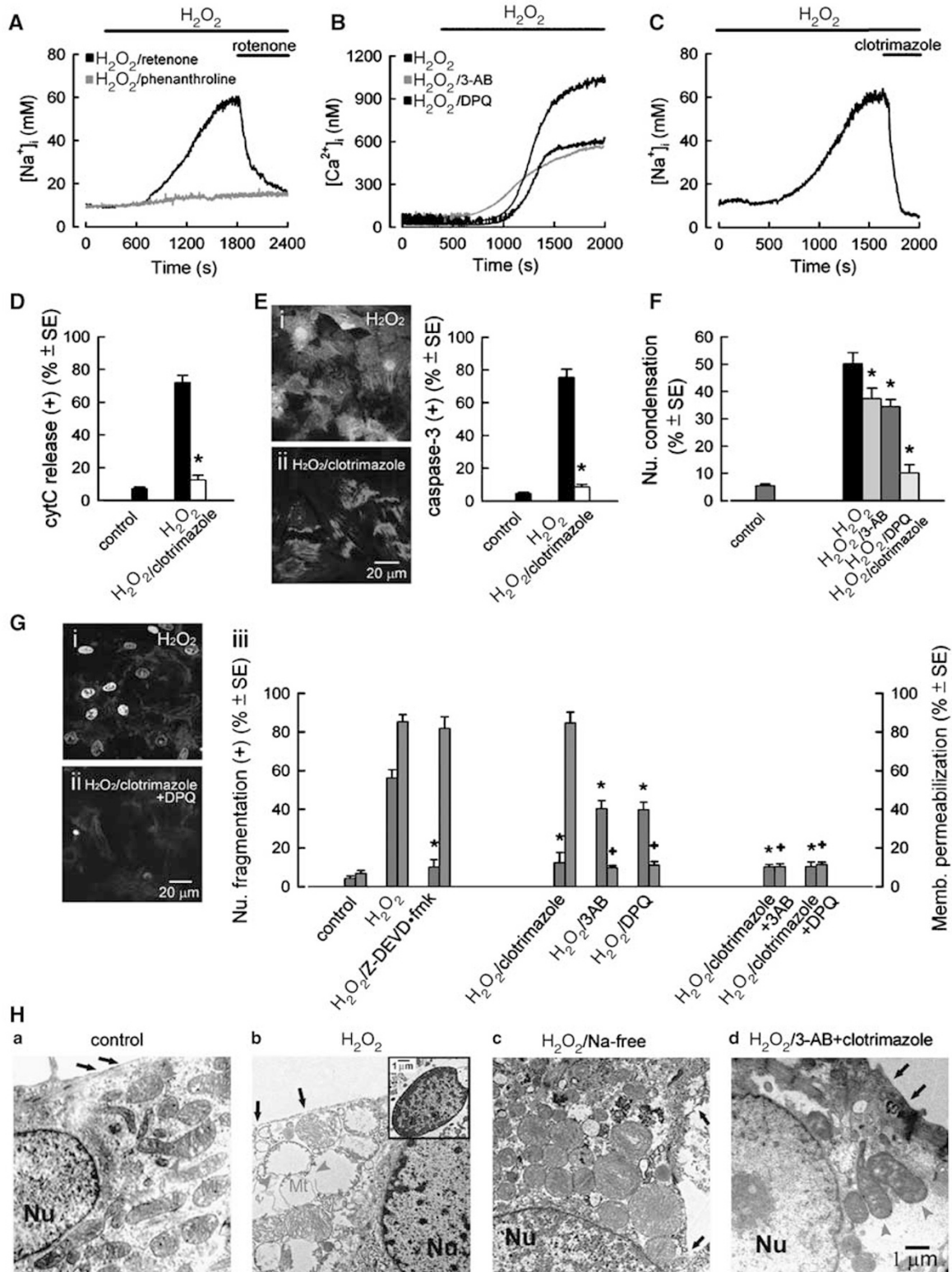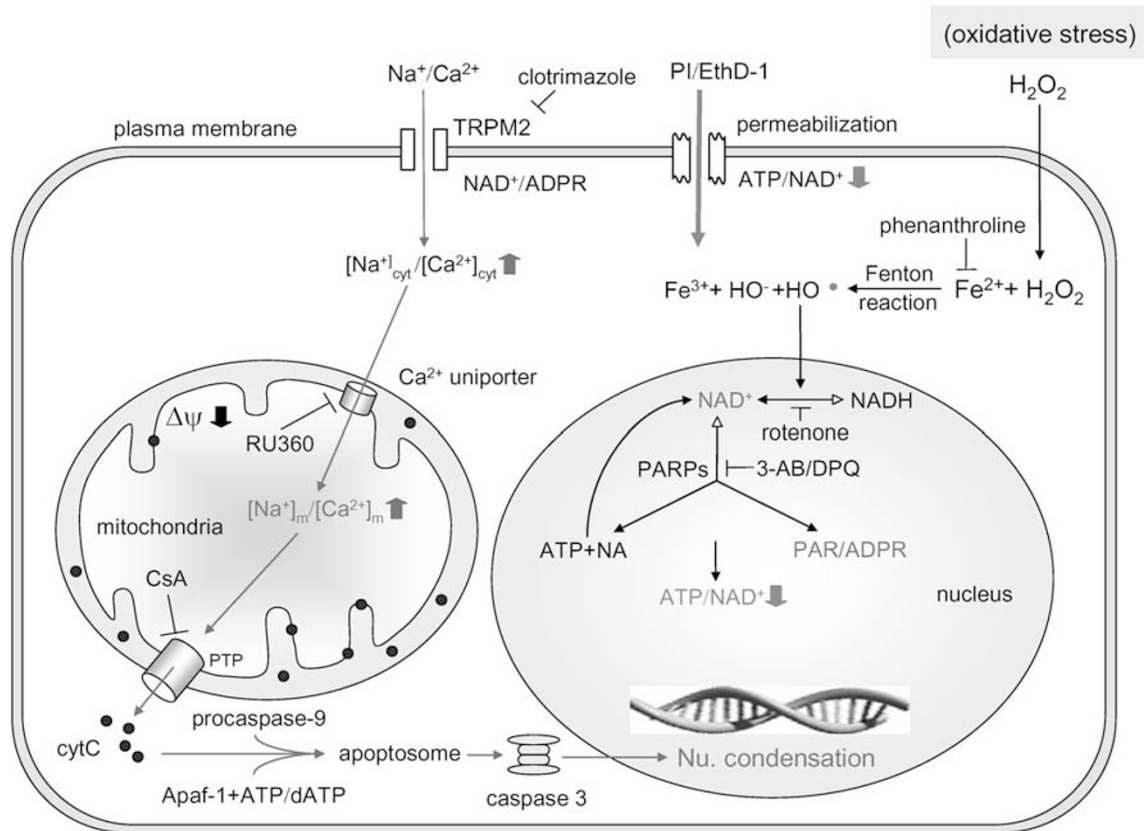
Figure 6 Possible molecular mechanism for H_2O_2-induced myocyte death. $OH^\bullet$ induces an increase in $NAD^+/ADPR$ levels, resulting in an early TRPM2 opening, followed by $[Na^+]_m/[Ca^{2+}]_m$ overload, which induces CsA-sensitive PTP opening,[4,11,33] apoptosome formation, and caspase 3-dependent nuclear condensation/fragmentation. Intracellular ATP/NAD^+ are also depleted, due to NAD^+ re-synthesis from ATP and nicotineamide (NA),[13] resulting in membrane permeabilization and DNA fragmentation/condensation in a single myocyte

Na-free medium; Supplementary Figure S3Biii) was still present.

Discussion

After I/R insult, untypical apoptotic and necrotic ultrastructural features are both seen in the heart and brain.[17–19] To our knowledge, this is the first report describing the molecular mechanisms involved in the two sets of death features in the same cell.

TRPM2 mRNA has been demonstrated in the heart.[25,26] We here provide the first evidence that functional TRPM2 channels are present in the myocyte plasmalemma (Supplementary Figures S1 and S2). Firstly, a TRPM2 protein was expressed (Supplementary Figure S2D). Secondly, the electrophysiological properties seen following exposure to the specific TRPM2 messengers, NAD^+ and ADPR, were very similar (Supplementary Figures S1 and S2) to those seen in TRPM2-expressing cell lines.[22–24,41] Moreover, a putative TRPM2 inhibitor, clotrimazole,[42] completely inhibited the ADPR-induced current (Supplementary Figure S2Ab).

We also provided four lines of evidence that H_2O_2 activates TRPM2 via an increase in $NAD^+/ADPR$ levels, resulting in the $[Ca^{2+}]_i/[Na^+]_i/Na^+]_m$ overload. Firstly, after exposure to H_2O_2, intracellular levels of NAD^+ and PAR/ADPR (see below) increased rapidly (Figure 1). Secondly, the electro-

physiological properties of the H_2O_2-induced currents (Supplementary Figure S3) were very similar to those induced using specific TRPM2 messengers (Supplementary Figures S1 and S2). Thirdly, clotrimazole, a putative TRPM2 inhibitor, inhibited both the TRPM2-/ADPR-induced currents (Supplementary Figure S2Ab) and the H_2O_2-induced Na^+/Ca^{2+} influx (Figure 5C). Fourthly, a decrease in the levels of both NAD^+ and PAR by either phenanthroline (Figure 1B) or rotenone (Figure 6) completely inhibited the Na^+/Ca^{2+} influx (Figure 5A), while complete inhibition of an increase in PAR/ADPR levels by 3-AB or DPQ (Figure 1Ed) had only a partial inhibitory effect on Ca^{2+}/Na^+ influx (Figure 3f and 5B). Our results therefore indicate that both NAD^+ and ADPR are involved in TRPM2 opening (Figure 6).

As reported by others,[25] we showed that the TRPM2 was opened by mono(ADPR) (Supplementary Figure S2Ab). Since anti-PAR antibody only recognizes polymer (Figure 1D),[32] it is difficult to know whether, following H_2O_2 exposure, mono(ADPR) levels increase, resulting in TRPM2 opening. When DNA is damaged by H_2O_2, the accumulated PAR undergoes rapid turnover, with a half-life of less than 1 min, and is converted into mono(ADPR) by PARG.[13,30,31] The partial inhibitory effect of 3-AB/DPQ on the Na^+/Ca^{2+} influx (Figure 5B) therefore suggests that mono(ADPR) is probably produced by PARG, resulting in TRPM2 opening. However, other explanations cannot be ruled out.

One important finding is that TRPM2 opening, resulting in the Na^+/Ca^{2+} overload, is involved in the H_2O_2-activated apoptotic machinery. There is evidence that ROS-induced $[Ca^{2+}]_m$ overload is one of the major causes of myocyte apoptosis.[4,11] However, under Ca-free conditions, in which the $[Ca^{2+}]_m$ overload should be totally abolished, nuclear condensation was only inhibited by $\sim 18\%$ (Figure 2g). In addition to the $[Ca^{2+}]_m$ overload, the H_2O_2-induced $[Na^+]_m$ overload also plays an essential role in the activation of the apoptotic machinery, since (i) at least 50% of the $[Ca^{2+}]_i$ overload originated from the H_2O_2-induced $[Na^+]_i$ overload (Supplementary Figure S3Af), and Ca-free treatment did not inhibit either the $[Na^+]_i$ overload (Supplementary Figure S3Ag) or the $[Na^+]_{cyt}/[Na^+]_m$ overload (Figure 2e), indicating that $[Na^+]_i$ overload is an important upstream signal for $[Ca^{2+}]_i$ overload; (ii) when H_2O_2-/Na-ionoph-induced $[Na^+]_m$ overload, but not $[Na^+]_{cyt}$ overload, was abolished, significant inhibition of nuclear condensation was seen (Figure 2g); and (iii) the EM study showed that Na-free treatment largely prevented the H_2O_2-induced mitochondrial membrane rupturing (Figure 5Hc), which results in Na-sensitive cytC release.

High concentrations of ROS/H_2O_2 induce PARP activation and $[ATP]_i/NAD^+$ depletion, leading to cardiac necrosis, and the use of PARP$^{-/-}$ mice or PARP inhibitors reduces the infarct area (necrosis) by ~ 20–25%,[13–15] indicating that other mechanisms may be involved (see below). EM analysis shows that the infarct area exhibits both necrotic and apoptotic changes,[17,18] which are very similar to those seen in the present study (Figure 5Hb). The present study showed that PARP inhibitors completely inhibited the *caspase 3-independent* necrotic changes (Figure 3g), but had only a small protective effect (~ 15–20%, Figure 5F and Giii) on the caspase 3-dependent nuclear changes. The coactivation of the caspase-dependent and -independent cell death machineries clearly showed that different mechanisms are involved (Figure 6). One possible explanation is that caspase 3 activation occurs earlier than depletion of $[ATP]_i$ (and NAD^+) and PI influx (Figure 4c), and the $[ATP]_i$ is therefore high enough for apoptosome formation to induce the apoptotic characteristics.[12,40] Since PARP is normally cleaved/inactivated by activated caspase 3,[13] we may ask why 3-AB-sensitive (Figure 3g), PARP-induced $[ATP]_i$ depletion still occurred after 40 min exposure to H_2O_2 (Figure 4c). One possible explanation is that maximum PARP activation (i.e. the peak level of PAR, Figure 1Ed) was seen as early as after 5–10 min exposure to H_2O_2, before caspase 3 activation, which started at 15 min and peaked at 30–40 min (Figure 4c). Since the resting level of the $[ATP]_i$ is ~ 4–7 mM in the heart,[43] it may take time (~ 40 min exposure, Figure 4c) for it to be completely depleted by activated PARP. It should be noted that PARP/PAR activity starts to slowly decrease after 30 min exposure (Figure 1Ed), at the time when caspase 3 activity peaked (~ 30–40 min exposure, Figure 4c).

Another important finding is that when TRPM2 and PARP activities were both inhibited by cotreatment with clotrimazole and 3-AB/DPQ, both the ultrastructural and microscopic changes of the two sets of death features were largely prevented (Figure 5G and Hd), showing a better protective effect ($>90\%$) than that seen when only PARP activity is inhibited (20–25%).[13–15] Further animal studies are needed to elucidate the therapeutic potential of the combination of PARP inhibitors and the widely used antifungal drug, clotrimazole, in providing better protection against I/R-induced injury.

Materials and Methods

Details of the following can be accessed in the expanded Methods section in Supplementary Materials: chemicals, external, and internal solutions; patch-clamp techniques; measurement of intracellular levels of NADH/NAD^+, $[Na^+]_i/[Ca^{2+}]_i$, and ATP ($[ATP]_i$); immunochemical detection of PAR and TRPM2; *in situ* examination of apoptosis or necrosis; and EM.

Preparation of neonatal rat ventricular myocytes

All procedures were performed in accordance with the Animal Care Guidelines of the National Taiwan University. In brief, 1-day-old Wistar rats (both sexes) were killed by cervical dislocation, then decapitated, and ventricular myocyte cultures prepared as described previously.[44]

Simultaneous measurement of $[Na^+]_{cyt}$ and $[Na^+]_m$ changes in a single ventricular myocyte using time-lapse confocal microscopy

The detailed method is described in Supplementary Materials. A Leica SP confocal laser-scanning imaging system equipped with a $63\times$ nicotinamide (NA) 1.32 oil immersion objective was used. The following equations[33] were used in Figure 2 to convert the F/F_0 ($F_0 =$ basal fluorescence) into the $[Na^+]_{cyt}$ or $[Na^+]_m$, respectively:

(1) $[Na^+]_{cyt} = 27.02 \, [F/F_0] - 18.65$ (correlation coefficient $= 0.998$)
(2) $[Na^+]_m = 43.47 \, [F/F_0] - 36.95$ (correlation coefficient $= 0.997$)

Statistics

In fluorescence measurement, all results are expressed as the mean $\pm$ S.E.M. for the stated number of animal preparations (n), each tested in duplicate. In immunostaining experiments, 200 cells from 10 randomly selected fields were scored on each coverslip; at least four animal preparations were used ($n = 4$) and duplicated in each test. Statistical differences were compared using the Mann–Whitney U-test, taking a P-value of <0.05 as significant.

Acknowledgements

References

1. Bolli R, Mohamed OJ, Patel BS, Aruoma OI, Halliwell B, Lai EK and McCay PB (1989) Marked reduction of free radical generation and contractile dysfunction by antioxidant therapy began at the time of reperfusion: evidence that myocardial 'stunning' is a manifestation of reperfusion injury. Circ. Res. 65: 607–622

2. Colucci WS (1997) Molecular and cellular mechanisms of myocardial failure. Am. J. Cardiol. 80: 15L–25L

3. Saraste A, Pulkki K, Kallajoki M, Henriksen K, Parvinen M and Voipio-Pulkki L-M (1997) Apoptosis in human acute myocardial infarction. Circulation 95: 320–323

4. Crow MT, Mani K, Nam Y-J and Kitsis RN (2004) The mitochondrial death pathway and cardiac myocyte apoptosis. Circ. Res. 95: 957–970

5. Horwitz LD, Fennessey PV, Shikes RH and Kong Y (1994) Marked reduction in myocardial infarct size due to prolonged infusion of an antioxidant during reperfusion. Circulation 89: 1792–1801

6. Matsumura K, Jeremy RW, Schaper J and Becker LC (1998) Progression of myocardial necrosis during reperfusion of ischemic myocardium. Circulation 97: 795–804

7. Leist M and Jäättelä M (2001) Four deaths and a funeral: from caspases to alternative mechanisms. Nat. Mol. Cell Biol. 2: 1–10

8. Green D and Kroemer G (1998) The central executioners of apoptosis: caspases or mitochondria? Trends Cell Biol. 8: 267–271

9. Petronilli V, Penzo D, Scorrano L, Bernardi P and Di Lisa F (2001) The mitochondrial permeability transition, release of cytochrome *c* and cell death. J. Biol. Chem. 276: 12030–12034

10. Newmeyer DD and Ferguson-Miller S (2003) Mitochondria: releasing power for life and unleashing the machineries of death. Cell 112: 481–490

11. Suleiman M-S, Halestrap AP and Griffiths EJ (2001) Mitochondria: a target for myocardial protection. Pharmacol. Ther. 89: 29–46

12. Leist M, Single B, Castoldi AE, Kuhnle S and Nicotera P (1997) Intracellular adenosine triphosphate (ATP) concentration: a switch in the decision between apoptosis and necrosis. J. Exp. Med. 185: 1481–1486

13. Virág L and Szabó C (2002) The therapeutic potential of poly(ADP-ribose) polymerase inhibitors. Pharmacol. Rev. 54: 375–429

14. Bowes J, McDonald MC, Piper J and Thiemermann C (1999) Inhibitors of poly(ADP-ribose) synthetase protect rat cardiomyocytes against oxidant stress. Cardiovasc. Res. 41: 126–134

15. Pieper AA, Walles T, Wei G, Clements EE, Verma A, Snyder SH and Zweier JL (2000) Myocardial postischemic injury is reduced by polyADPribose polymerase-1 gene disruption. Mol. Med. 6: 271–282

16. Buja LM and Entman ML (1998) Modes of myocardial cell injury and cell death in ischemic heart disease. Circulation 98: 1355–1357

17. Ohno M, Takemura G, Ohno A, Misao J, Hayakawa Y, Minatoguchi S, Fujiwara T and Fujiwara H (1998) Apoptotic myocytes in infarcts area in rabbit hearts may be oncotic myocytes with DNA fragmentation: analysis by immunogold electron microscopy combined with *in situ* nick end-labeling. Circulation 98: 1422–1430

18. Dumont EAWJ, Hofstra L, van Heerde WL, van den Eijnde S, Doevendans PAF, DeMuinck E, Daemen MARC, Smits JFM, Frederik P, Wellens HJJ, Daemen MJAP and Reutelingsperger CPM (2000) Cardiomyocyte death induced by myocardial ischemia and reperfusion: measurement with recombinant human annexin-V in a mouse model. Circulation 102: 1564–1568

19. Van Lookeren Campagne M and Gill R (1996) Ultrastructural morphological changes are not characteristic of apoptotic cell death following focal cerebral ischemia in the rat. Neurosci. Lett. 213: 111–114

20. Montell C, Birnbaumer L and Flockerzi V (2002) The TRP channels, a remarkably functional family. Cell 108: 595–598

21. Clapham DE (2003) TRP channels as cellular sensors. Nature 426: 517–524

22. Hara Y, Wakamori M, Ishii M, Maeno E, Nishida M, Yoshida T, Yamada H, Shimizu S, Mori E, Kudoh J, Shimizu N, Kurose H, Okada Y, Imoto K and Mori Y (2002) LTRPC2 Ca^{2+}-permeable channel activated by changes in redox status confers susceptibility to cell death. Mol. Cell 9: 163–173

23. Wehage E, Eisfeld J, Heiner I, Jüngling E, Zitt C and Lückhoff A (2002) Activation of the cation channel long transient receptor potential channel 2 (LTRPC2) by hydrogen peroxide: a splice variant reveals a mode of activation independent of ADP-ribose. J. Biol. Chem. 277: 23150–23156

24. McHugh D, Flemming R, Xu S-Z and Perraud A-L (2003) Critical intracellular Ca^{2+} dependence of transient receptor potential melastatin 2 (TRPM2) cation channel activation. J. Biol. Chem. 278: 11002–11006

25. Perraud A-L, Fleig A, Dunn CA, Bagley LA, Launay P, Schmitz C, Stokes AJ, Zhu Q, Bessman MJ, Penner R, Kinet J-P and Scharenberg AM (2001) ADP-ribose gating of the calcium-permeable TRRPC2 channel revealed by nudix motif homology. Nature 411: 595–599

26. Sano Y, Inamura K, Miyake A, Mochizuki S, Yokoi H, Matsushime H and Furuichi K (2001) Immunocyte Ca^{2+} influx system mediated by LTRPC2. Science 293: 1327–1330

27. Nieminen A-L, Byrne AM, Brian H and Lemasters JJ (1997) Mitochondrial permeability transition in hepatocytes induced by t-BuOOH: NAD(P)H and reactive oxygen species. Am. J. Physiol. 272: C1286–C1294

28. Filipovic DM, Meng X and Reeves B (1999) Inhibition of PARP prevents oxidant-induced necrosis but not apoptosis in LLC-PK1 cells. Am. J. Physiol. 277: F428–F436

29. Ying W, Sevigny MB, Chen Y and Swanson RA (2001) Poly(ADP-ribose) glycohydrolase mediated oxidative and excitotoxic neuronal death. Proc. Natl. Acad. Sci. USA 98: 12227–12232

30. Alvarez-Gonzalez R and Althaus FR (1989) Poly(ADP-ribose) catabolism in mammalian cells exposed to DNA-damaging agents. Mutat. Res. 218: 67–74

31. D'amours D, Desnoyers S, D'silva I and Poirier GG (1999) Poly(ADP-ribosyl)ation reactions in the regulation of nuclear functions. Biochem. J. 342: 249–268

32. Küpper JH, de Murcia G and Bürkle A (1990) Inhibition of poly(ADP-ribosylation) by overexpressing the poly(ADP-ribose) polymerase DNA-binding domain in mammalian cells. J. Biol. Chem. 265: 18721–18724

33. Yang K-T, Pan S-F, Chien C-L, Hsu S-M, Tseng Y-Z, Wang S-M and Wu M-L (2004) Mitochondrial Na^+ overload is caused by oxidative stress and leads to activation of the caspase 3-dependent apoptotic machinery. FASEB J. 12: 1442–1444

34. Chen Z, Alcayaga C, Suárez-Isla BA, O'Rourke B, Tomaselli G and Marbán E (2002) A 'minimal' sodium channel construct consisting of ligated S5-P-S6 segments forms a toxin-activatable ionophore. J. Biol. Chem. 277: 24653–24658

35. Chen W-H, Chu K-C, Wu S-J, Wu J-C, Shui H-A and Wu M-L (1999) Early metabolic inhibition-induced intracellular sodium and calcium increase in rat cerebellar granule cells. J. Physiol. (London) 515: 133–146

36. Collins TJ, Lipp P, Berridge MJ and Bootman MD (2001) Mitochondrial Ca^{2+} uptake depends on the spatial and temporal profile of cytosolic Ca^{2+} signals. J. Biol. Chem. 276: 26411–26420

37. Matlib MA, Zhou Z, Knight S, Ahmed S, Choi KM, Krause-Bauer J, Philips R, Altschuld R, Katsube Y, Sperelakis N and Bers DM (1998) Oxygen-bridged dinuclear ruthenium amine complex specifically inhibits Ca uptake into mitochondria *in vitro* and *in situ* in single cardiac myocytes. J. Biol. Chem. 273: 10223–10231

38. Gincel D, Zaid H and Shoshan-Barmatz V (2001) Calcium binding and translocation by the voltage-dependent anion channel: a possible regulatory mechanism in mitochondrial function. Biochem. J. 358: 147–155

39. McConkey DJ (1998) Biochemical determinants of apoptosis and necrosis. Toxicol. Lett. 42: 123–130

40. Jacobson MD, Weil M and Raff MC (1996) Role of Ced-3/ICE-family proteases in staurosporine-induced programmed cell death. J. Cell Biol. 133: 1041–1051

41. Zhang W, Chu X, Tong Q, Cheung JY, Conrad K, Masker K and Miller BA (2003) A novel TRPM2 isoform inhibits calcium influx and susceptibility to cell death. J. Biol. Chem. 278: 16222–16229

42. Hill K, McNulty S and Randall AD (2004) Inhibition of TRPM2 channels by the antifungal agents clotrimazole and econazole. Naunyn-Schmiedeberg's Arch. Pharmacol. 370: 227–237

43. Allen DG, Morris PG, Orchard CH and Pirolo JS (1985) A nuclear magnetic resonance study of metabolism in the ferret heart during hypoxia and inhibition of glycolysis. J. Physiol. (London) 361: 185–204

44. Wu M-L, Chen C-C and Su M-J (2000) Possible mechanism(s) of arachidonic acid-induced intracellular acidosis in rat cardiac myocytes. Circ. Res. 86: e55–e62

Supplementary Information accompanies the paper on Cell Death and Differentiation website (http://www.nature.com/cdd)